# Edge-wicking: Micro-fluidics of two-dimensional liquid penetration into porous structures

**Hanna Wiklund and Tetsu Uesaka**

**KEYWORDS:** Micro-fluidics, Edge-wicking, Porous structure, Lattice Boltzmann

**SUMMARY:** We have performed free-energy-based two-dimensional lattice Boltzmann simulations of the penetration of liquid into the edge of a porous material. The purpose was to gain further insight into possible mechanisms involved in the penetration of liquid into the unsealed edges of paper and paper board. In order to identify the fundamental mechanisms we have focused on a model structure that consists of a network of interconnected capillaries. Two different mechanisms were identified: pinning at corners of solid surfaces and increased pressure in dead-end pores. These mechanisms significantly decelerate or even stop the liquid penetration into the porous structures.

**ADDRESSES OF THE AUTHORS: Hanna Wiklund** (hanna.wiklund@miun.se), **Tetsu Uesaka** (tetsu.uesaka@miun.se) , Mid Sweden University, Holmgatan 10, SE-851 70 Sundsvall, Sweden

**Corresponding author: Hanna Wiklund**

Edge wicking or the penetration of liquid into the unsealed edges of paper and paper board is widely seen in various converting operations and end-use. Understanding the fundamental mechanisms that control liquid penetration into random porous structures and quantifying the effects of paper and liquid properties, such as contact angle and surface tension is important when, for example, designing paper board suitable for liquid packaging.

The problems have been investigated by many researchers mainly by using experimental approaches. The penetration of liquids into paper has been shown to be determined by capillary forces, external pressures, and in the case of aqueous liquids, diffusion into fibre walls that will cause swelling, increase in volume, of the fibres (Lyne 1984). It has been known for many years that the relative importance of each mechanism is influenced by the structure of the sheet and the amount and chemical composition of the sizing agent. In very dense and hard sized paper board the liquid penetrates not by capillary action into pores but through diffusion into fibres (Bristow 1971). Later studies have found that if an external pressure is present the structure becomes important (Salminen 1988).

Tufvesson et al. used near-infrared spectroscopy in combination with multivariate analysis to measure in-plane wetting in board (Tufvesson et al. 2007). They have studied the effect of sizing and paper structure but also the effect of heated water and edge wicking in samples exposed to saturated steam (Tufvesson, Lindström 2007). Their results confirmed previous results, boards with a lower level of sizing and lower density showed larger edge wicking than other boards, but they also showed that the effect of board density became insignificant in boards when placed on a cooling plate and exposed to saturated steam.

The Lucas-Washburn equation has often been used to model liquid transport into porous structures. Various adjustments have been made to take into account structural effects, such as tortuosity and porosity (Lepoutre 1978), but also the effect of dynamic contact angle, which has been shown to increase as the velocity of the liquid contact line increases (Rose, Heins 1962; Siebold et al. 2000). In cellulosic structures it is well known that aqueous liquids will cause swelling, increase in volume, of the fibres. Chatterjee has suggested that if the swelling is instantaneous the basic relationships in the Washburn equation should not be changed except for the introduction of a radius that represents the radius of a wet capillary. However, if the swelling is instead slow, as in the case of a highly swellable type of fibre, the Lucas – Washburn equation is not valid because of the continuous change in the fibre dimensions (Chatterjee 1985).

Other studies have shown that at longer time-scales the liquid penetration deviates from Lucas-Washburn behaviour. Lindström et al. studied the imbibition of water, under the influence of gravity, into laminated paper grades with a wide range of porosities (Lindström et al. 2011). They found two regimes; an initial Lucas-Washburn regime with the characteristic $t^{1/2}$ time-dependence and a second long time-scale regime where the capillary intrusion is logarithmic in time. The latter regime was explained in terms of a thermally activated process, which has its origin in molecular kinetics theory for contact line dynamics.

Although the Lucas-Washburn equation in many cases may describe the overall behaviour of liquid penetration, it is still a phenomenological description when applied to random porous media. First, the real random porous structures have no smooth, chemically homogeneous and continuous cylindrical pores. Second, the pore structures are *multi-scale*, ranging from large inter-fibre pores to fibres between fibrils. At these length scales it is difficult, if not impossible, to perform systematic experiments.

The main advantage of numerical simulations is the possibility of setting up experiments with full control over both geometric and wetting effects and where each phenomenon can be studied one at a time, in order to better understand the fundamental mechanisms that determine the penetration of liquids into random porous structures.

In this work we focus our study on the effects of micro structures, particularly micro-topography, on liquid penetration driven by capillary force. For this purpose we set up a model structure that consists of a network of interconnected capillaries to investigate specific structural effects. We use a lattice Boltzmann method for binary fluids (Briant, Yeomans 2004; Pooley et al. 2008)

to solve the dynamic equations for this two-phase flow problem.

## Materials and Methods

### Simulation set-up

*Fig 1* shows a cross section picture of paper board taken by scanning electron microscope (SEM). The pore structure in paper and paper board is typically characterized by pores that are (more or less) interconnected and oriented in the in-plane direction. These pore-channels changes their diameters along the length, sometimes merge with other channels, create a "throat", or are partially closed (dead-end pore channels). In addition, the surfaces of the solids (fibres) are not smooth, often showing "corners". Although using the system in *Fig 1* directly in simulation, with some coarse-grained procedures, may give a good picture of the overall behaviour of the penetration of liquid it is difficult to extract information on how the different individual structural properties of the system have the ability to speed up, slow down or, in some cases, even stop liquid penetration. Therefore, in order to identify and separate specific structure effects, we instead created the following model structures, as shown in *Fig 2*. In both figures, the capillaries are more or less oriented in the in-plane direction, but possess discontinuities. The corners are also present on the solid surfaces. *Figure 2b* contains a few dead-end pores; otherwise it is the same as *Fig 2a*. It is important to note that these features are the ones that are missing in the Lucas-Washburn model capillaries but are present in real random porous structures.

The basic assumption of this simulation model is that the pore structure is static (or not dynamic), i.e. it doesn't change its size and shape as the liquid penetrates the structure, such as in the case of swelling. Another assumption is that the solid surfaces are chemically homogeneous, and therefore, there is no variation of static contact angle.

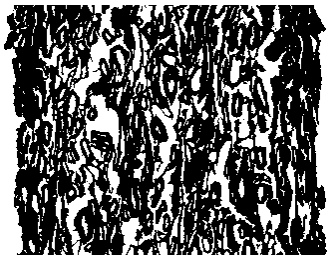

Fig 1. SEM-image of paper structure

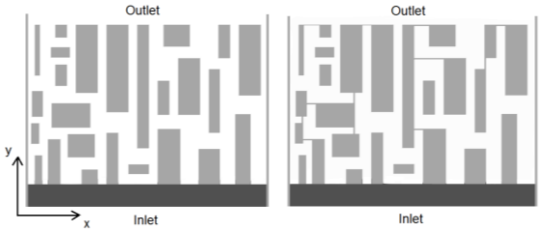


(a) (b)

Fig 2. Schematic of simulation set up. a) Open and b) partially closed structure. Dark grey areas represent the liquid-phase, white the air-phase and light grey the solid surfaces.

### Simulation model

In this study we consider the penetration of liquid into random porous structures as a binary flow problem, that is, the flow of liquid/air. To describe the binary fluid system we have used a diffuse interface model developed by Cahn and Hilliard. In the Cahn-Hilliard model, it is assumed that the local free energy density of a binary fluid is a function of composition and composition gradient. To take wetting surfaces into account, Cahn introduced a surface energy term (Cahn 1977). Assuming that the solid surface-fluid interfacial energy is a function of only the fluid composition at the solid surface, the equilibrium properties of such a solid-binary fluid system can be described by a free energy functional (Cahn 1977; Briant, Yeomans 2004; Papatzacos 2000)

$$\Psi = \Psi_b + \Psi_s = \int_V \left( \psi_b(C) + \frac{\kappa}{2} \partial_\alpha C \partial_\alpha C \right) dV + \int_S \psi_s(C) dS \qquad [1]$$

where $\psi_b(C)$ is the bulk free energy density and $\psi_s(C)$ is a surface free energy density function. $C$ is the order parameter, to distinguish the two phases, and is a measure of the amount of phase, i.e. the concentration. The gradient term in *Eq 1* represents the contribution from the fluid-fluid interface. κ is a constant related to the surface tension and α represents the Cartesian coordinates. In order to model the immiscibility of the two fluids $\psi_b(C)$ is taken to be (Briant, Yeomans 2004)

$$\psi_b(C) = \frac{1}{3}\rho \ln \rho + A\left( -\frac{1}{2}C^2 + \frac{1}{4}C^4 \right) \qquad [2]$$

where ρ is the average fluid density and A is a constant. This choice of bulk free energy density has a double well structure with minima at $C = \pm 1$ corresponding to the two stable phases of the fluids. At equilibrium, the concentration profile both at the solid surface and in the bulk must minimize the total free energy, *Eq 1*. In other words, from the calculus of variations, the concentration profile $C$ must first satisfy

$$\frac{\partial \Psi}{\partial C} = \frac{\psi_b}{\partial C} - \kappa\left(\partial_\alpha^2 C\right) = \mu_{chem} = const. \qquad [3]$$

and second the natural boundary condition (Papatzacos 2000):

$$\partial_\perp C = \frac{1}{\kappa} \frac{\partial \psi_s}{\partial C} \qquad [4]$$

where $\mu_{chem}$ is the chemical potential and $\partial_\perp C$ denotes the derivative in the direction normal to the solid surface and into the domain. The choice of *Eq 2* for $\psi_b$, and setting the right hand side of *Eq 3* to zero yields an interface with surface tension, σ and interface width, ξ (Briant, Yeomans 2004):

$$\sigma = \sqrt{8\kappa A/9}\,, \quad \xi = \sqrt{\kappa / A} \qquad [5]$$

The choice of surface free energy density function is very important for accurately capturing the physics of wetting

(Wiklund et al. 2011). It was shown in our previous study that in order for $\psi_s$ to satisfy *Eqs 3* and *4* a cubic function is necessary and the following expression can be found (Wiklund et al. 2011):

$$\psi_s(C) = \sqrt{\frac{\kappa A}{2}}\cos\theta\left(\frac{1}{3}C^3 - C\right) + const. \quad [6]$$

The dynamics is governed by the continuity equation, the Navier-Stokes equations, and the convection-diffusion equation (Briant Yeomans 2004; Pooley et al. 2008):

$$\partial_t \rho + \partial_\alpha(\rho u_\alpha) = 0 \quad [7]$$

$$\partial_t(\rho u_\beta) + \partial_\alpha(\rho u_\beta u_\alpha) = -\partial_\alpha P_{\alpha\beta} + \partial_\alpha\{\upsilon\rho(\partial_\beta u_\alpha + \partial_\alpha u_\beta)\} \quad [8]$$

$$\partial_t C + \partial_\alpha(C u_\alpha) = M\nabla^2\mu_{chem} \quad [9]$$

where $\bar{u}$ is the velocity, $M$ is the mobility, and $\upsilon$ is the kinematic viscosity. The thermodynamic properties of the system enter the hydrodynamic description through the chemical potential $\mu_{chem}$ and the pressure tensor $P_{\alpha\beta}$. The pressure tensor can be found from the free energy functional and is given by (Briant, Yeomans 2004; Pooley et al. 2008)

$$P_{\alpha\beta} = p\delta_{\alpha\beta} + \kappa\partial_\alpha C\partial_\beta C \quad [10]$$

where

$$p = p_0 - \kappa C\partial_\alpha^2 C - \frac{\kappa}{2}\partial_\alpha C\partial_\alpha C \quad [11]$$

$$p_0 = \frac{1}{3}\rho + A\left(-\frac{1}{2}C^2 + \frac{1}{4}C^4\right) \quad [12]$$

To solve the above equations we use a lattice Boltzmann numerical scheme (Briant, Yeomans 2004) together with a wetting boundary condition for diffuse interface models (Wiklund et al. 2011; Papatzacos 2000). The lattice Boltzmann method solves the Navier-Stokes equations by following the evolution of particle velocity distribution functions on a fixed regular lattice. Interfaces between the two fluids are modelled through a scalar phase field, and the model makes specific tracking of surfaces unnecessary and therefore there are no assumptions of the specific shape of the interface.

We use the binary free energy lattice Boltzmann model, first developed by Swift et al. (Swift et al. 1996) and later extended by Briant et al. (Briant, Yeomans 2004 ) and Pooley et al. (Pooley et al. 2008). The binary free energy lattice Boltzmann model includes two particle distribution functions $f_i(\bar{r},t)$ and $g_i(\bar{r},t)$ where $\bar{r}$ denotes the position in the lattice and $i$ is the lattice direction. In this work, we use a two dimensional lattice with directions denoted $\bar{e}_0 = (0,0)$, $\bar{e}_{1,3} = (\pm1,0)$, $\bar{e}_{2,4} = (0,\pm1)$, $\bar{e}_{5,7} = (\pm1,\pm1)$, and $\bar{e}_{6,8} = (\mp1,\pm1)$. The distribution functions are updated through

$$f_i(\bar{r} + \bar{e}_i\Delta t, t + \Delta t) = f_i(\bar{r},t) - \frac{1}{\tau_f}\left(f_j - f_j^{eq}\right) \quad [13]$$

$$g_i(\bar{r} + \bar{e}_i\Delta t, t + \Delta t) = g_i(\bar{r},t) - \frac{1}{\tau_g}\left(g_j - g_j^{eq}\right) \quad [14]$$

where $\Delta t$ is the time step and $f_j^{eq}$ and $g_j^{eq}$ are the equilibrium distribution functions, and they determine the equilibrium properties of the system. $\tau_f$ and $\tau_g$ are the relaxation parameters as described later.

$f_i(\bar{r},t)$ is related to the macroscopic fluid density ρ and momentum $\rho\bar{u}$ and $g_i(\bar{r},t)$to the order parameter C:

$$\rho = \sum_i f_i \quad [15]$$

$$\rho\bar{u} = \sum_i f_i\bar{e}_i \quad [16]$$

$$C = \sum_i g_i \quad [17]$$

where $\bar{e}_i$ denotes the lattice velocity vector. The relaxation parameters $\tau_f$ and $\tau_g$ are related to the kinematic viscosity, ν, and mobility, M, through

$$\nu = \frac{1}{3}\left(\tau_f - \frac{1}{2}\right) \quad [18]$$

$$M = \Gamma\left(\tau_g - \frac{1}{2}\right) \quad [19]$$

where $\Gamma$ is a diffusion coefficient. In our simulations the mobility was chosen as M=0.5, the grid resolution as 1 μm per 2 lattice units, and the interface width as ξ=1. The model has been validated in a previous study (Wiklund et al. 2011) using droplet-spreading and capillary-rise as test cases. The model with this choice of parameter values was shown to accurately capture the capillary intrusion phenomena for a wide range of contact angles. The relative error between the measured and simulated contact line velocity was less than 8 %, even for small capillaries.

Boundary conditions are implemented by putting constraints on the distribution functions $f_i(\bar{r},t)$and $g_i(\bar{r},t)$ such that they satisfy a no-slip boundary condition and the wetting boundary condition in *Eq 4* at solid boundaries, and a mass conservation condition at the inlet and outlet.

## Results

We have performed simulations of liquid penetration into the two different structures in *Fig 2* varying the contact angles of the solid surfaces. The surface tension was set to 0.073 N/m and the viscosity of the liquid-phase is about ten times that of the air-phase. No gravity. Initially the bottom part of the system is filled with the liquid phase while the model structure is filled with the air-phase. The liquid is then allowed to penetrate the structure through capillary forces, no external pressure is applied. The percentage of penetrated liquid into the structure is recorded as a function of time.

*Fig3* shows the percentage of penetrated liquid into the structures as a function of square root of time for two different equilibrium contact angles, θ=20° and θ=60°. In all cases tested, after some small penetration delay, there is an initial regime where the penetration follows the typical $t^{1/2}$ (Lucas-Washburn) behaviour. This behaviour is governed by a force balance dominated by the capillary pressure and the hydrodynamic drag. At a later time in the simulation all curves deviate from this behaviour. In a majority of the cases tested the penetration of liquid into the structure stops. However, in the case of the open structure with θ=20° the penetration doesn't stops but instead the curve exhibits a series of "bumps", suggesting that in some places in the structure the penetration at some point slows down and later accelerates.

In order to investigate the underlying mechanisms behind the behaviour seen in *Fig 3* we look at snapshots of the liquid penetration, comparing the phase field and the relative pressure field. The relative pressure is defined as the ratio of the pressure to the pressure at inlet (or outlet).

In *Figs 4* and *5* snapshots of the liquid penetration into the open structure is shown at different times in the simulation for θ=60° and θ=20° respectively. It is obvious that the initial regime, with a Lucas-Washburn type behaviour, comes from the fact that the structure initially consists of a number of smooth capillaries.

It is also clear from *Fig 4* that for the case θ=60° the liquid front stops when it reaches the part where the structure opens up and the sharp corners in the structure pins the contact line. At the time when the liquid front stops, the curvature of the interface between the two phases is lost, see (A). A loss of the curvature of the interface means that there is no longer any capillary pressure driving the liquid front further. Looking at the pressure field plot this can indeed be seen.

It can also be seen in *Fig 5b* that if the structure is more complex, with more horizontal features close to the liquid interface, see point (C), then the pressure increases. Compare with point (D), where there are no horizontal obstacles close to the interface. This pressure increase causes a resistance to the penetration of the liquid.

In *Fig 6* snapshots of the liquid penetration into the partially closed structure is shown at different times, for θ=20°. Here, contrary to the case with the open structure, the liquid front stops. The contact line is again pinned at the crners.

Comparing *Figs 5b* and *6b,* of the pressure field at different times for the two different structures with θ=20°, we find a significant difference in the pressure distribution between the open and partially closed structures. An increase in the pressure is clearly visible in the dead-end capillaries of the partially closed structure. The pressure increase created in the dead-end capillaries obviously prevents the liquid from moving further in the structure.

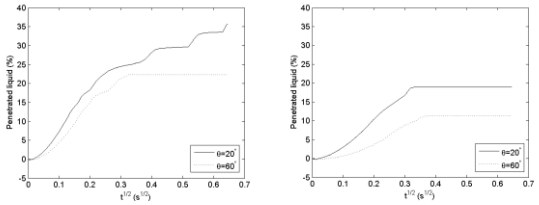

Fig 3. The percentage of penetrated liquid as a function of square root of time. a) Open and b) partially closed structure.

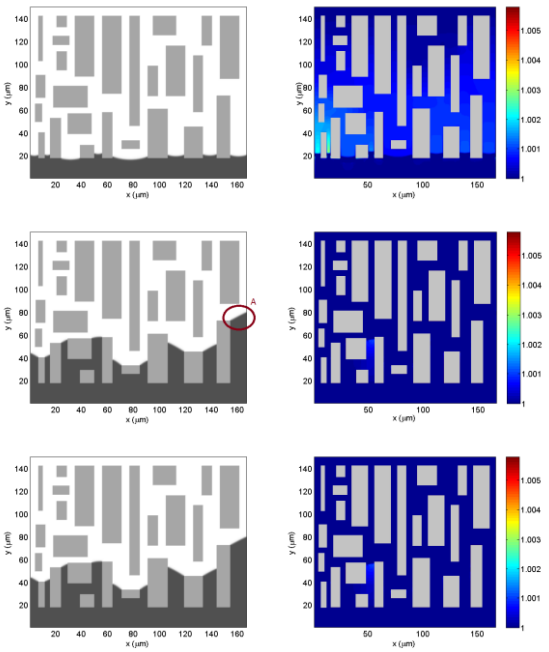

a) b)

Fig 4. Snapshots of the liquid penetration into the open structure is shown at different times in the simulation for θ=60°. a) Phase-field and b) relative pressure-field.

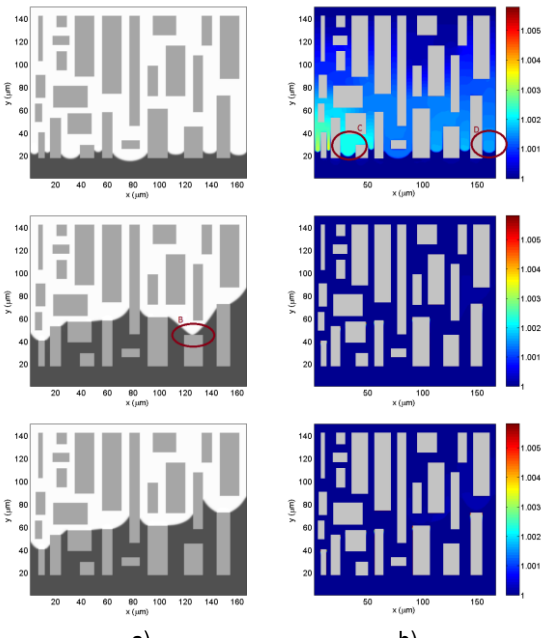

a) b)

Fig 5. Snapshots of the liquid penetration into the open structure is shown at different times in the simulation for θ=20°. a) Phase-field and b) relative pressure-field.

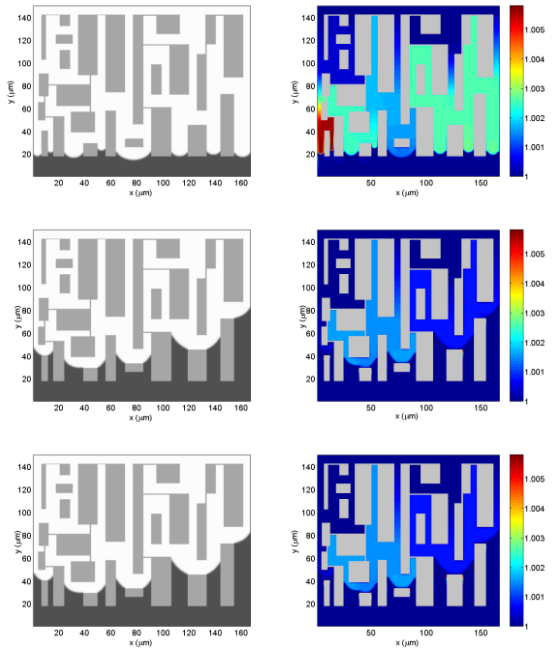

a) b)

Fig 6. Snapshots of the liquid penetration into the partially closed structure is shown at different times in the simulation for θ=20°. a) Phase-field and b) relative pressure-field.

## Discussion

We have been able to identify two mechanisms related to the microscopic structure that either prevent or slow down the penetration of liquid into a porous structure. Pinning results in a loss of curvature and a subsequent loss in capillary pressure that causes the penetration to stop and an increase in the pressure in dead-end pores that in some cases even prevent the liquid from entering the structure. It is however important to point out that a major challenge when dealing with numerical simulations of patterned structures is to handle boundary conditions correctly. In this work we have used a wetting boundary condition that defines the concentration value in the normal direction from a flat surface. At corners no such exact result is available. In this case we have solved this by calculating the boundary condition in each direction outward from the corner and then taking the average as the boundary value at corners. However, pinning at corners is not just a numerical artefact but is a well known and real phenomenon (de Gennes et al. 2003). Pinning has also been experimentally observed, both on geometrically and chemically heterogeneous substrates (Yamanaka et al. 2004; Kugori et al. 2008). In fact the pinning result we obtained very much followed the model described in (de Gennes et al. 2003; Kugori et al. 2008).

One important question is why the results presented here showed a very limited amount of penetration of liquid, whereas penetration continues much further in real paper structures. One explanation is that, as mentioned earlier, real paper structures have continuous solid (fibre) surfaces that will lead the liquid front by capillary forces, whereas the model structures we employed have discontinuities in the form of sharp corners. The latter amplifies the effects of pinning. Another obvious point is that the model investigated here is two-dimensional, while real paper is three-dimensional and has a much more interconnected and continuous structure, promoting wicking. One last point is swelling, which was not included in this study but will also have an impact on the liquid penetration. Therefore, the results obtained here are still of semi-quantitative nature. Despite this limitation, these results give an important insight on how to prevent edge-wicking, by altering the internal structures of paper. Creating the distracted, discontinuous structures with sharp corners is not difficult, for example, by imbedding inorganic pigments in the edges of paperboard.

## Conclusions

We have performed numerical simulations of liquid penetration into model structures. The structure consists of a network of interconnected capillaries. In some cases the capillaries are closed in one end. We varied the contact angle of the surfaces in the structures. Our results showed that at a macroscopic level the penetration of a liquid into a porous structure is very much dependent on the micro-structure details. Pinning can occur at sharp corners and can slow down or even stop the penetration in some cases. An increase in pressure caused by dead-end capillaries in the structure will prevent and slow down the penetration. Traditionally edge-wicking is controlled by porosity and contact angle from the point of paper structure. The results in this study may, however, suggest an alternative way of controlling edge-wicking: including cornered objects (fillers) and creating a small number of dead-end pores.

### Literature

**Briant A. J. and Yeomans J. M.** (2004): Lattice Boltzmann simulations of contact line motion. II. Binary fluids, Phys. Rev. E 69(3), 1603.

**Bristow J. A.** (1971): The swelling of paper during the sorption of aqueous liquids, Svensk Papperstidning, 74(20), 645

**Cahn J. W.** (1977): Critical point wetting, J. Chem. Phys. 66(8), 3667.

**Chatterjee P. K.** (1985): Mechanisms of liquid flow and structureproperty relationships. In: P. K. Chatterjee (ed.) Absorbency, number 7 in Textile Science and Technology, chapter 2, Elsevier, NY, pp. 29-84

**de Gennes P.G., Brochard-Wyart F. and Quere D.** (2003): Capillarity and Wetting phenomena: Drops, Bubbles, Pearls, Waves, Springer, New York, (Chapter 9).

**Kugori K., Yan H. and Tsujii K.** (2008): Importance of pinning effect of wetting in super water-repellent surfaces. Colloids and Surfaces A: Physiochem. Eng. Aspects 317, 592.

**LePoutre P.** (1978): Liquid absorption and coating porosity, Paper Technol. 19, 298.

**Lindström S. B., Cervin N. T and Wågberg L.** (2011): Thermally activated capillary intrusion of water into cellulose fiber-based materials. In Proceedings of the Fundamental and Applied Pulp and Paper Modeling Symposium. 2011

**Lyne M. B.** (1984): Wetting and penetration of aqueous liquids, In Mark, R. E. (ed.), Handbook of Physical and Mechanical

Testing of Paper and Paperboard, Mercel Dekker Inc. New York, pp. 103-121.

**Papatzacos P**. (2000): Macroscopic Two-phase Flow in Porous Media Assuming the Diffuse-interface Model at Pore-level, Transp. Porous Media 49(2), 139.

**Pooley C. M., Kusumaatmaja H. and Yeomans J. M.** (2008): Contact line dynamics in binary lattice Boltzmann simulations, Phys. Rev. E 78(5), 6709.

**Rose W. and R. W. Heins** (1962): Moving interfaces and contact angle rate-dependency, J. Colloid Sci., 17(1), 39

**Salminen P.** (1988): Studies of water transport in paper during short contact time, PhD thesis, Laboratory of Paper Chemistry Department of Chemical Engineering, Åbo Akademi, Finland.

**Siebold A, Nardin M, Schultz J, Walliser A, and Oppliger M.** (2000): Effect of dynamic contact angle on capillary rise phenomena, Coll. And Surf. 161, 81.

**Swift M. R., Orlandini E., Osborn W. R. and Yeomans J. M.** (1996): Lattice Boltzmann Simulations of liquid-gas and binary fluid systems. Phys. Rev. E 54(5), 5041.

**Tufvesson H., Eriksson S., Lindström T.** (2007): Determination of the in-plane wetting of a board structure using NIR spectroscopy, Nord. Pulp Paper Res. J. 22(1), 111.

**Tufvesson H., Lindström T.** (2007): The effect of sizing and paper structure on paperboard for retortable packaging, Nord. Pulp Paper Res. J. 22(2), 200.

**Wiklund H., Lindström S. B. and Uesaka T.** (2011): Boundary condition considerations in lattice Boltzmann formulations, Comp. Phys. Comm. 182, 2192.

**Yamanaka M., Okada A. and Kawai A.** (2004): Pinning effect of microliquid drop on geometrical complex substrates composed with different surface energy materials. J. Vac. Sci Technol. B 22(6), 3525.